JOURNAL OF CHEMICAL & ENGINEERING DATA

ARTICLE

pubs.acs.org/jced

Solubility and Phase Separation of 2-(*N*-Morpholino)ethanesulfonic Acid (MES) and 4-(*N*-Morpholino)butanesulfonic Acid (MOBS) in Aqueous 1,4-Dioxane and Ethanol Solutions

Mohamed Taha and Ming-Jer Lee*

Department of Chemical Engineering, National Taiwan University of Science and Technology, 43 Keelung Road, Section 4, Taipei 106-07, Taiwan

ABSTRACT: 2-(*N*-Morpholino)ethanesulfonic acid (MES) and 4-(*N*-morpholino)butanesulfonic acid (MOBS) are useful for pH control as standard buffers in the physiological range of 5.5 to 6.7 for MES and 6.9 to 8.3 for MOBS, respectively. The densities of MES and MOBS in water and in aqueous 1,4-dioxane and ethanol solutions were measured with a vibrating-tube digital densimeter at 298.15 K and concentrations up to saturated conditions. The solubilities of MES and MOBS at 298.15 K were determined in the mixed solvents of (1,4-dioxane + water) and (ethanol + water) using the experimental results of density measurements. MOBS shows liquid−liquid phase separation over the concentrations of 1,4-dioxane from 0.4 to 0.9 in mass fraction. The phase diagram of 1,4-dioxane + MOBS + water system was also determined experimentally at 298.15 K, including tie-lines in the two-liquid phase region. Binodal data were fitted to an empirical equation and the effective excluded volume (EEV) model. The reliability of the experimental tie-line data was confirmed by using the Othmer−Tobias and the Bancroft equations. Apparent free energies of transfer ($\Delta G'_{tr}$) of zwitterionic buffers from water to aqueous 1,4-dioxane and ethanol solutions have been calculated from the solubility data. The contribution of transfer free energies ($\Delta g'_{tr}$) of the ($-CH_2-CH_2-$) group from water to aqueous 1,4-dioxane and ethanol solutions was estimated from the $\Delta G'_{tr}$ results.

INTRODUCTION

Buffer systems are extremely important for solution chemistry. For instance, buffer solutions are used to calibrate pH meters and to maintain a stable pH value of a solution in which pH-dependent chemical reactions take place. The efficiency of many chemical separations and the rates of many chemical reactions are governed by the pH value of the solution. Buffer solutions can be used to control the reaction conditions and yields in organic syntheses. In industrial chemistry, the need for adequate pH control may be essential in determining the courses of precipitation reactions and of electrodeposition of metals. The consideration of hydrogen ion concentration is important parameter to control in numerous laboratory research techniques such as electrophoresis, chromatography, polarography, solvent extraction, and immunoassays. The pH balance is also an important in maintaining desirable aquatic ecological conditions in natural waters.

As it is clear, many enzyme-catalyzed reactions release and consume hydrogen ions, which can be neutralized by the incorporation of buffers that undergo reversible protonation. Good and his associates[1,2] described a group of buffers which were useful for many biological and chemical applications, covering the pK_a values between 6.1 and 8.4. Most of these buffers were zwitterionic, capable of possessing both positive and negative charges on the same molecule.

Good's buffers have several advantages; their buffering capacities are independent of temperature and concentration, and they are very soluble in water but poorly soluble in nonpolar solvents (fats, oils, and organic solvents), as this would tend to prevent the buffer compound to traverse cellular membranes or accumulate in nonpolar compartments in biological systems. Most of the pH measurements in biological systems are performed in the aqueous phase. However, sometimes mixed aqueous-water miscible solvents, such as ethanol and 1,4-dioxane, are used for dissolving compounds of biological importance. 2-(*N*-Morpholino)ethanesulfonic acid (MES) and 4-(*N*-morpholino)butanesulfonic acid (MOBS) are receiving widespread acceptance in many biological applications.[3−12] In fact, to our best knowledge, there are no solubility data of MES and MOBS in water or in organic solvents. In the present study, solubilities of MES and MOBS in water and in aqueous 1,4-dioxane and ethanol solutions have been determined experimentally at 298.15 K and atmospheric pressure. The phase diagram of 1,4-dioxane + MOBS + water system at 298.15 K is also reported. The solubility data were formed a basis to evaluate the apparent free energy of transfer ($\Delta G'_{tr}$) of these two buffers from water to aqueous 1,4-dioxane and ethanol solutions at 298.15 K. MES and MOBS are structurally related and differ only in the length of the alkane group side chain: the *N*-(morpholino)-alkane-sulfonic acids, containing ethane (in MES) or butane (in MOBS). The contribution of ($-CH_2-CH_2-$, Scheme 1) was predicted from the apparent free energies of transfer, $\Delta G'_{tr}$.

EXPERIMENTAL SECTION

MES (mass fraction purity >0.99) and MOBS (mass fraction purity >0.99) were purchased from Sigma Chemical Co. (USA).

Special Issue: Kenneth N. Marsh Festschrift

Received: March 29, 2011
Accepted: May 5, 2011
Published: May 16, 2011

Scheme 1. Schematic Illustration of the Contribution of the $(-CH_2-CH_2-)$ Group of MOBS

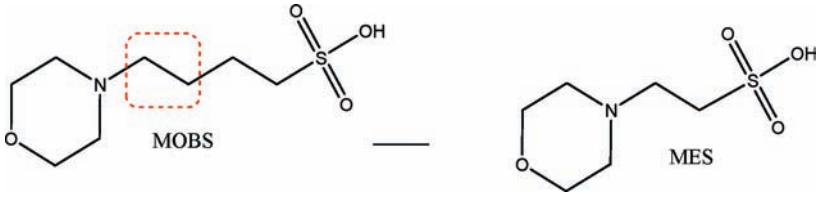

1,4-Dioxane (mass fraction purity >0.99) was purchased from Acros Organic (USA). Ethanol, 0.998 purity, was obtained from Sigma Chemical Co. (USA). All of the purchased materials were used without further purification. Water used for making the aqueous solutions was obtained from NANO pure-Ultra pure water system that was distilled and deionized with resistance of 18.3 MΩ.

Densities of the aqueous solutions were measured with an Anton Paar DMA 4500 vibrating tube densimeter, Austria. The uncertainty of the density measurement of the unsaturated and the saturated solutions is $\pm\ 5\cdot10^{-5}$ g·cm^{-3} and $\pm\ 2\cdot10^{-4}$ g·cm^{-3}, respectively. The densimeter has a built-in thermostat for maintaining the desired temperatures within a temperature range of (273.15 to 363.15) K. The apparatus calibration was performed periodically. Degassed water and air were used for calibration.

Solubilities of MES and MOBS in water and in aqueous 1,4-dioxane and ethanol solutions at 298.15 K were obtained from the density data, following the procedure of Liu and Bolen.[13] The detailed procedure used in this work has been delineated in our earlier articles.[14] The uncertainty of the solubility limit is lower than ± 0.8 % (relative value, S_B/mol·kg^{-1}).

The phase diagram (binodals) was constructed by the cloud point method.[15] From the stock, a fixed weight of solvent (0.4 to 0.9 1,4-dioxane in mass fraction) was filled into glass vials. MOBS (0.001 g, approximately) was added to the vials, to provide a series of mixtures with increasing composition of MOBS compound, until the mixture became turbid, which indicates the two-phase formation (LLE binodal). In a similar way by using solvent mixtures with various compositions, the experimental solid−liquid−liquid equilibrium (SLLE) phase boundary data were obtained by adding MOBS with increasing its composition to other sample vials until solid had appeared in the two liquid phases. The mixtures were prepared by weight using an electronic balance (R&D model GR-200) with a precision of ± 0.1 mg. Each vial was sealed with a Teflon coated screw cup. The vials were completely in a thermostatic shaker equipped with water bath (BT-350R, Yih-Der, Taiwan) at 298.15 K for at least 48 h, and then the phases were allowed to settle for 8 h. The transition point between the different regions was determined visually. The uncertainly of the phase boundary determination is estimated to be ± 0.0005 in mass fraction.

A glass vessel (10 cm^3) with an external jacket, in which water at constant temperature was circulated, was used to carry out the tie-line determination for the 1,4-dioxane + MOBS + water system at 298.15 K. The same experimental apparatus and methodology has been described in detail elsewhere.[16] The temperature of equilibrium cell was maintained constant using a thermostatic bath within ± 0.1 K. The cell's temperature was measured with a mercury thermometer calibrated by a precision thermometer (6, model 1560, Hart Scientific Co., USA) to an uncertainty of ± 0.1 K. The mixtures were agitated using a magnetic stirrer for 12 h at 298.15 K, and then the equilibrium phases were left 8 h at the studied temperature to settle down. A series of known weights of 1,4-dioxane, MOBS, and water lying within the two-phase region were introduced into the equilibrium cells. Then, samples from each phase were taken with a syringe. The compositions of 1,4-dioxane and water in both upper and lower phases were analyzed by a gas chromatography (model 9800, China Chromatography Co., Taiwan) equipped with a thermal conductivity detector (TCD). A 1.83 m long Porapak Q 80/100 column was utilized to separate 1,4-dioxane and water. The injection port and detector temperatures were kept at 513.15 K, while the oven temperature was held at 493.15 K. High purity helium (99.99 %) was used as a carrier gas at a flow rate 25 cm^3·min^{-1}. The injection volume of liquid samples was about 1 μL. The equilibrium compositions were determined from five replicated samples for each phase to acquire high accuracy. The solute (MOBS) cannot be allowed in the packed column or in the detector. To this purpose, a stainless tube packed with glass wools was used as a filter and was connected at the entry of the column. The filter should be replaced when a significant amount of buffer was trapped. The averaged area fraction from the gas chromatography analysis was converted into mole fraction via calibration equations. Calibrations were made with gravimetrically prepared binary samples within two composition ranges, in accordance with those in the organic-rich phase and the water-rich phase for the ternary system. The composition of MOBS in each phase was determined by acid−base titrations.

RESULTS AND DISCUSSION

Tables 1 and 2 report the determined densities (ρ) for the mixtures of MES or MOBS in water and in mixed solvents of (1,4-dioxane + water) or (ethanol + water) at 298.15 K and concentrations up to saturated conditions. The solubility limit of the zwitterionic buffers is determined at the point of intersection in a density plot as shown in Figure 1. The density versus composition data of the unsaturated solutions were fitted to a polynomial (from 2 to 4 degrees), while the densities of the saturated solutions were fitted to a horizontal line. The solubility limits (molal concentration) of MES and MOBS in 1,4-dioxane + water and in ethanol + water mixtures and the corresponding densities (ρ^*) of the saturated solutions at 298.15 K are listed in Table 3, and buffers' solubilities are also visualized in Figure 2. In all cases, the solubilities are significantly reduced by the presence of 1,4-dioxane or ethanol. It is generally not possible to accurately extend all solubility measurements of MES and MOBS to pure 1,4-dioxane or ethanol, because of extremely low solubility in these solvents. The solubility of MOBS is significantly higher than that of MES in pure water. The higher solubility is likely due

Table 1. Experimental Densities (ρ) of MES in Water and Aqueous 1,4-Dioxane and Ethanol Solutions (w_{diox} = Mass Fraction of 1,4-Dioxane; w_{EtOH} = Mass Fraction of Ethanol) at 298.15 K under Atmospheric Pressure

m	ρ	m	ρ	m	ρ
mol·kg^{-1}	g·cm^{-3}	mol·kg^{-1}	g·cm^{-3}	mol·kg^{-1}	g·cm^{-3}
water		w_{diox} = 0.1		w_{diox} = 0.2	
0.0912	1.00297	0.1267	1.01333	0.0797	1.01892
0.1344	1.00573	0.2633	1.02154	0.1898	1.02565
0.1940	1.00949	0.5189	1.03625	0.2650	1.03014
0.3209	1.01730	0.7555	1.04886	0.3884	1.03702
0.5911	1.03314	1.0198	1.06217	0.5277	1.04518
0.8494	1.04733	1.1375	1.06892	0.6374	1.05090
1.0651	1.05851			0.7561	1.05709
1.2723	1.06878			0.8924	1.06384
1.4396	1.07665				
w_{diox} = 0.3		w_{diox} = 0.4		w_{diox} = 0.5	
0.0456	1.02468	0.0774	1.03318	0.0361	1.03554
0.0774	1.02722	0.1157	1.03579	0.0812	1.03825
0.1627	1.03180	0.1706	1.03900	0.1376	1.04157
0.2250	1.03587	0.2227	1.04177	0.1910	1.04461
0.3151	1.04084	0.3140	1.04704	0.2244	1.04658
0.4320	1.04727	0.2514	1.04335		
0.5405	1.05304	0.3821	1.05067		
		0.4275	1.05307		
w_{diox} = 0.6		w_{diox} = 0.7		w_{diox} = 0.8	
0.0087	1.03696	0.0018	1.03709	0.0006	1.03560
0.0151	1.03744	0.0052	1.03728	0.0012	1.03567
0.0328	1.03817	0.0054	1.03744	0.0016	1.03572
0.0363	1.03855	0.0065	1.03765	0.0022	1.03575
0.0540	1.03944	0.0144	1.03786	0.0040	1.03585
0.0627	1.04048	0.0186	1.03808	0.0143	1.03655
0.0825	1.04140	0.0220	1.03848	0.0066	1.03603
0.0975	1.04235	0.0286	1.03891	0.0090	1.03620
0.1136	1.04324	0.0366	1.03942	0.0114	1.03635
		0.0404	1.03967		
w_{EtOH} = 0.1		w_{EtOH} = 0.2		w_{EtOH} = 0.3	
0.1622	0.99047	0.0615	0.97033	0.0336	0.95337
0.2738	0.99731	0.1371	0.97524	0.0844	0.95643
0.3974	1.00421	0.2686	0.98341	0.1621	0.96184
0.5378	1.01315	0.4040	0.99162	0.2260	0.96533
0.6441	1.01919	0.5459	0.99975	0.2739	0.96829
0.7970	1.02744	0.6751	1.00703	0.3346	0.97210
0.9120	1.03322			0.4056	0.97619
1.0243	1.03898			0.4895	0.98087
w_{EtOH} = 0.4		w_{EtOH} = 0.5		w_{EtOH} = 0.6	
0.0368	0.93431	0.0309	0.91275	0.0364	0.89020
0.0871	0.93756	0.0412	0.91315	0.0476	0.89107
0.1403	0.94141	0.0808	0.91598	0.0616	0.89186
0.2005	0.94471	0.1012	0.91726	0.0807	0.89320
0.2791	0.94962	0.1341	0.91939	0.0933	0.89393
0.3096	0.95174	0.1606	0.92089	0.1043	0.89458
		0.1776	0.92204		

Table 1. Continued

m	ρ	m	ρ	m	ρ
mol·kg^{-1}	g·cm^{-3}	mol·kg^{-1}	g·cm^{-3}	mol·kg^{-1}	g·cm^{-3}
w_{EtOH} = 0.7		w_{EtOH} = 0.8			
0.0184	0.86498	0.0042	0.83981		
0.0259	0.86550	0.0078	0.84007		
0.0328	0.86604	0.0100	0.84022		
0.0408	0.86656	0.0119	0.84038		
0.0508	0.86727	0.0140	0.84053		
0.0603	0.86794	0.0159	0.84067		

to the presence of two more CH_2 group in MOBS molecule between the sulfate and the protonated amine group. Similar trends were observed[14,17] when comparing the solubility of *N*-tris(hydroxymethyl)methyl-4-aminobutanesulfonic acid (TABS) in water with that of [(2-hydroxy-1,1-bis(hydroxymethyl)ethyl)-amino]-1-propanesulfonic acid (TAPS). The methylene groups decrease the intramolecular interactions between the sulfate and the protonated amine groups, which observed from the crystal structure of some zwitterionic buffers.[18,19]

Molecular interactions in a ternary system are usually more complicated than those in a binary system. The solute may have affinity either to the two solvent species or one of them. Moreover, there are interactions between the solvent molecules themselves. For instance, if the force of the solute is far stronger for the one than for the other solvent, a redistribution of the solvent molecules may occur around the solute molecules resulting that the solvent as a whole can no longer be considered a uniform medium.[20] The MOBS-induced phase separation of 1,4-dioxane + water system takes place in a similar manner as for the 1,4-dioxane + water + TABS system,[17] in a range of 1,4-dioxane concentration, 0.4 to 0.9 in mass fraction (mole fraction, x_{diox}, 0.12 to 0.65). MOBS and TABS are highly water-soluble solutes but extremely insoluble in the organic solvents. In the water-rich region (x_{diox} < 0.1) the water−water hydrogen-bonded network is predominant, and 1,4-dioxane molecules are probably embedded into the water network;[21] thus, 1,4-dioxane and MOBS molecules are completely hydrated with water molecules and formed a homogeneous liquid phase. As 1,4-dioxane is added, the water structure becomes less ordered.[21] Concerning the question of what forces cause this process of phase separation, there does not exist any somehow reasonable explanation, unless one arbitrarily attributes to the high affinity of these solutes to form strong hydrogen bonds with water molecules. These hydrogen-bonding forces overcome the forces between water and 1,4-dioxane molecules, and then 1,4-dioxane molecules are excluded from the water network. The phase separation suggests that 1,4-dioxane can be used as an antisolvent for the crystallization of MOBS.

A phenomenon may be interesting that buffer-induced phase separation (buffering-out), as shown in Figure 3. This figure shows a photograph of the separated phases at certain concentration of MOBS at room temperature. 1,4-Dioxane is miscible with water at any composition, and a clear solution is obtained. The color is due to disperse blue 14 dyestuff, which is soluble in 1,4-dioxane and practically insoluble in water.

Table 4 presents the experimental phase boundary data obtained for the 1,4-dioxane + MOBS + water system at 298.15 K. The phase diagram of this ternary system is shown

Table 2. Experimental Densities (ρ) of MOBS in Water and Aqueous 1,4-Dioxane and Ethanol Solutions (w_{diox} = Mass Fraction of 1,4-Dioxane; w_{EtOH} = Mass Fraction of Ethanol) at 298.15 K under Atmospheric Pressure

m / mol·kg^{-1}	ρ / g·cm^{-3}	m / mol·kg^{-1}	ρ / g·cm^{-3}	m / mol·kg^{-1}	ρ / g·cm^{-3}
water		w_{diox} = 0.1		w_{diox} = 0.2	
0.1108	1.00391	0.1483	1.01440	0.0990	1.01982
0.2292	1.01104	0.2845	1.02216	0.2163	1.02650
0.5267	1.02763	0.8908	1.05319	0.3394	1.03325
0.7999	1.04172	1.5317	1.08069	0.8800	1.06066
1.7143	1.08133	2.3839	1.11015	1.3990	1.08214
2.3105	1.10272	3.2724	1.13512	1.9000	1.09909
3.1109	1.12671	4.1610	1.15522	2.4127	1.11828
3.7289	1.14233	4.6721	1.16717	3.1253	1.13971
4.4694	1.15870			3.8416	1.15568
5.0273	1.16982			4.3582	1.16534
5.5090	1.17839				
5.7375	1.18233				
w_{diox} = 0.3		w_{EtOH} = 0.1		w_{EtOH} = 0.2	
0.173	1.03198	0.1619	0.99059	0.1842	0.97843
0.313	1.03970	0.4073	1.00505	0.3472	0.98844
0.5437	1.05213	0.8975	1.03152	0.8480	1.01597
0.9163	1.06949	1.7032	1.06720	1.3517	1.03984
1.6091	1.09710	2.7349	1.10204	1.7859	1.05856
2.1053	1.11680	3.3430	1.11961	2.4424	1.08237
2.6509	1.13650	4.1475	1.14205	3.1626	1.10447
2.9078	1.14564	4.9722	1.16150	3.9426	1.12489
3.2028	1.15569	5.2999	1.16632	4.5943	1.14029
w_{EtOH} = 0.3		w_{EtOH} = 0.4		w_{EtOH} = 0.5	
0.1550	0.96115	0.2391	0.94722	0.0917	0.91649
0.4329	0.97811	0.7488	0.97685	0.1800	0.92236
1.1439	1.01607	1.2405	1.00157	0.2936	0.92980
1.2795	1.02239	1.4735	1.01238	0.6277	0.94982
2.0175	1.05355	1.7674	1.02543	0.8807	0.96270
2.3827	1.06752	2.2129	1.04135	1.1512	0.97770
2.9138	1.08457	2.5284	1.05393	1.4578	0.99291
3.3541	1.09998	2.9014	1.06649	1.7370	1.00539
3.8406	1.11050			1.9402	1.01397
				2.1715	1.02246
w_{EtOH} = 0.6		w_{EtOH} = 0.7		w_{EtOH} = 0.8	
0.0331	0.88968	0.0359	0.86695	0.0368	0.84297
0.1038	0.89454	0.1096	0.87181	0.0574	0.84421
0.1816	0.89985	0.1670	0.87563	0.0794	0.84539
0.3397	0.91013	0.2252	0.87979	0.0931	0.84652
0.6251	0.92786	0.3209	0.88612	0.1077	0.84748
0.9064	0.94375	0.4089	0.89177	0.1195	0.84833
1.0484	0.95136	0.4745	0.89629		
1.2106	0.95987				
1.3313	0.96589				
w_{EtOH} = 0.9					
0.0013	0.81408				
0.0022	0.81415				
0.0044	0.81428				
0.0083	0.81454				
0.0127	0.81483				
0.0160	0.81506				
0.0192	0.81526				

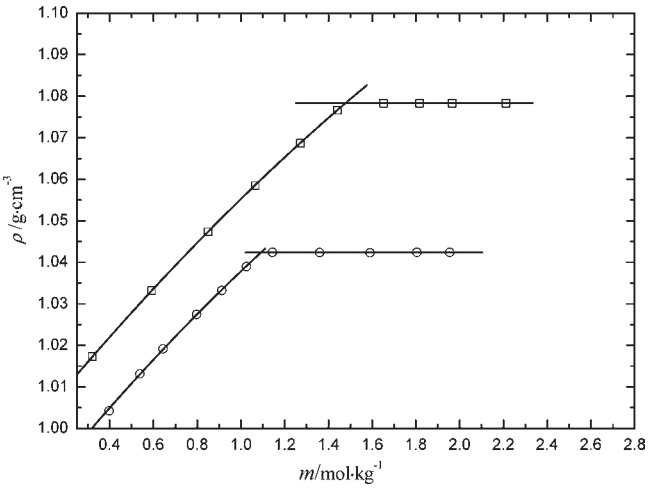

Figure 1. Representative density profiles of MES in water and 0.1 mass fraction of ethanol at 298.15 K: □, water; ○, 0.1 mass fraction of ethanol. The symbol m is the composition of buffer in solvents at 298.15 K under atmospheric pressure.

in Figure 4, where they are divided into five phase regions. The letters L and S refer to the liquid phase and the solid phase, respectively. Ignoring the existence of vapor phase, we mark L on the phase diagram to represent the homogeneous region of unsaturated solution. The biphasic region is labeled 2L. Three tie-lines were also shown in this region. The three-phase (S + 2L) region is composed of the saturation of the two liquid phases with MOBS solid. There are two liquid−solid regions (S + L), one with a liquid rich in water and MOBS (Figure 4, right) and another with a liquid rich in 1,4-dioxane and trace amount of MOBS (Figure 4, left). The right branch of the SLE phase boundary represents the solubility limits (mass fractions) measured by the densimetry method.

The binodal data of the aqueous 1,4-dioxane−MOBS system were correlated with the following empirical equation:

$$w_1 = a + bw_2^{0.5} + cw_2 + dw_2^3 \quad (1)$$

where w_1 and w_2 refer to the mass fractions of 1,4-dioxane and MOBS buffer, respectively. The coefficients a, b, c, and d along with the corresponding standard deviations (SD) for the binodal LLE data are determined from regression, and the results are collected in Table 5. The values of the parameters b and d are set to be zero for correlating the SLE and the SLLE phase boundary data (Table 5). The correlated results are also shown in Figure 4 (solid lines). On the basis of obtained standard deviations, we conclude that eq 1 is able to accurately reproduce the phase boundaries.

Table 3. Solubilities (S_B) of MES and MOBS in Aqueous 1,4-Dioxane and Ethanol Solutions and Densities (ρ_B^*) at Solubility Limits at 298.15 K

	S_B/mol·kg^{-1}				ρ_B^*/g·cm^{-3}			
	1,4-dioxane		ethanol		1,4-dioxane		ethanol	
$(w_{org.solv})^a$	MES	MOBS	MES	MOBS	MES	MOBS	MES	MOBS
0	1.48	5.91	1.48	5.91	1.0783	1.1876	1.0783	1.1876
0.1	1.22	5.32	1.10	5.61	1.0713	1.1807	1.0425	1.1701
0.2	0.945	4.57	0.756	4.95	1.0666	1.1701	1.0114	1.1479
0.3	0.635	3.36	0.533	4.04	1.0585	1.1602	0.9836	1.1190
0.4	0.450	phase separation	0.332	3.33	1.0541	phase separation	0.9529	1.0791
0.5	0.254		0.199	2.23	1.0482		0.9235	1.0251
0.6	0.123		0.115	1.42	1.0438		0.8953	0.9697
0.7	0.044		0.066	0.533	1.0399		0.8683	0.9001
0.8	0.016		0.017	0.125	1.0366		0.8408	0.8488
0.9				0.021				0.8154

[a] $w_{org.solv}$ = mass fraction of organic solvent.

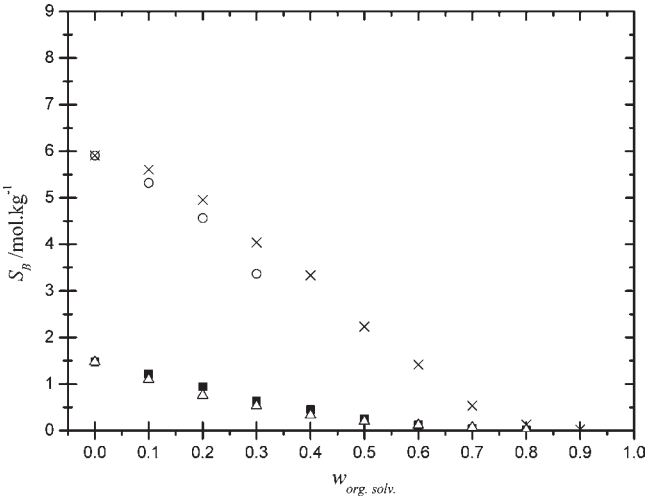

Figure 2. Solubility limits of MES and MOBS in water and in aqueous 1,4-dioxane and ethanol solutions at 298.15 K: MES (■) and MOBS (○) in aqueous 1,4-dioxane solutions; MES (△) and MOBS (×) in aqueous ethanol solutions; $w_{org.solv}$ = mass fraction of organic solvent.

The scaled effective excluded volume (EEV) of MOBS was calculated using the model developed by Guan et al.[22] This theory was used to correlate binodal data of polymer−polymer system. Recently, the applications of this model on hydrophilic alcohol−salt[23−25] and ionic liquid−salt[26,27] systems were demonstrated. The EEV equation for 1,4-dioxane + MOBS + water system can be written as

$$w_1 = -ln\left(V_{213}^* \frac{w_2}{M_2} + f_{213}\right)\frac{M_1}{V_{213}^*} \qquad (2)$$

where w_1 and w_2 represent the mass fractions of 1,4-dioxane and MOBS buffer, respectively; M_1 and M_2 are the molar mass of the 1,4-dioxane (88.11 g·mol^{-1}) and MOBS (223.29 g·mol^{-1}), respectively; V_{213}^* is the scaled effective excluded volume; and the parameter f_{213} is the volume fraction of unfilled effective available volume after tight packing of MOBS molecules into the network of 1,4-dioxane molecules in its aqueous solution. The V_{213}^* and

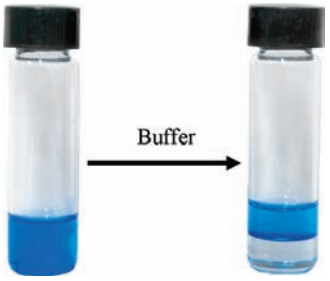

Figure 3. Photographs of buffer-out phase separation behavior of the 1,4-dioxane + MOBS + water system. The color is due to disperse blue 14 dyestuff.

f_{213} values obtained from the correlation of the experimental binodal LLE data are 245.803 g·mol^{-1} and 0.0945, respectively. The corresponding standard deviation (SD) is 0.023, which indicates that the EEV model gives a satisfactory result. The dashed line in Figure 4 is a fit to the experimental binodal LLE data using the EEV model.

For aqueous 1,4-dioxane−MOBS system the tie-line compositions at 298.15 K are given in Table 6 and presented in Figure 4. MOBS buffer is utilized to induce the liquid−liquid phase separation and is concentrated in the more dense, lower phase, whereas 1,4-dioxane is concentrated in the less dense, upper phase. 1,4-Dioxane is a widely used solvent in paints, varnishes, lacquers, cosmetics, and deodorants as well as in pharmaceutical industries. Similar to other water-miscible organic solvents, for example, ethanol, propanol, and isopropanol, 1,4-dioxane forms azeotrope with water, which is a barrier of recovery of pure 1,4-dioxane from its aqueous solutions by the distillation method. Therefore, the separation of high-purity 1,4-dioxane from its aqueous solution is of particular interest to industrial chemists and process engineers. This buffer (MOBS) can be used as an auxiliary agent to recover 1,4-dioxane from the azeotropic aqueous solution with the aid of liquid−liquid phase splitting.

The reliability of experimentally measured tie-line data was also ascertained by the Othmer−Tobias (eq 3) and Bancroft

dx.doi.org/10.1021/je200244p |J. Chem. Eng. Data 2011, 56, 4436–4443

Table 4. Phase Boundary Data as Mass Fraction (w_i) for the Ternary System 1,4-Dioxane (1) + MOBS (2) + Water (3) at 298.15 K under Atmospheric Pressure

w_1	w_2	w_3	w_1	w_2	w_3	w_1	w_2	w_3
One Liquid Phase + One Solid Phase[a]			Two Liquid Phases			Two Liquid Phases + One Solid Phase		
0	0.5689	0.4311	0.2945	0.3236	0.3819	0.2373	0.4067	0.3560
0.0457	0.5429	0.4114	0.3689	0.2222	0.4089	0.2792	0.3726	0.3482
0.0990	0.5048	0.3962	0.4922	0.1291	0.3787	0.3175	0.3580	0.3245
0.1653	0.4490	0.3857	0.6621	0.0472	0.2907	0.4335	0.2774	0.2891
			0.7451	0.0251	0.2298	0.5387	0.2111	0.2502
			0.8431	0.0054	0.1515	0.7381	0.0774	0.1845
						0.8400	0.0090	0.1510

[a] Solubility limits as mass fraction.

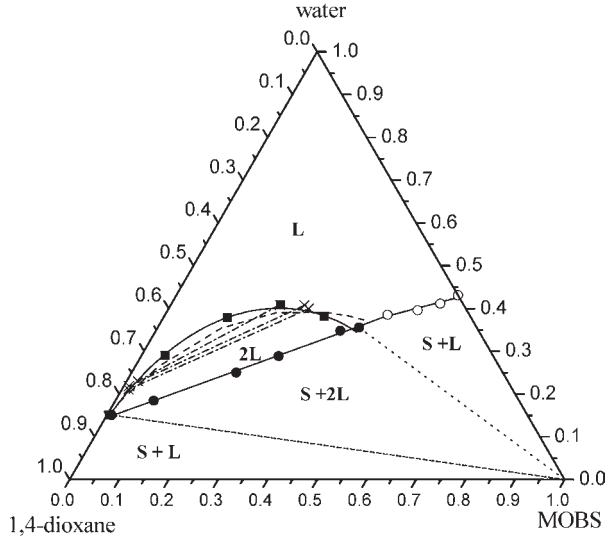

Figure 4. Phase diagram of MOBS in aqueous solutions of 1,4-dioxane (in mass fraction) at 298.15 K. The symbols ○, ●, and ■ represent, respectively, the solid solubility data of MOBS before liquid phase separation (SLE), binodal data of SLLE curves, and binodal data of LLE curves. Solid lines show the calculated results from eq 1, while dashed lines show the calculated values from eq 2. The tie lines are shown in the two-liquid-phase region (dash−dot lines).

(eq 4) equations.[28]

$$\frac{1-w_1^{II}}{w_1^{II}} = k_1\left(\frac{1-w_2^{I}}{w_2^{I}}\right)^n \quad (3)$$

$$\frac{w_3^{I}}{w_2^{I}} = k_2\left(\frac{w_3^{II}}{w_1^{II}}\right)^r \quad (4)$$

where w_1^{II}, w_2^{I}, w_3^{I}, and w_3^{II} are the equilibrium compositions (in mass fraction) of 1,4-dioxane (1), MOBS (2), and water (3) in top (II) and bottom (I) phases, respectively. The parameters k_1, k_2, n, and r are the fitting parameters, and their values are 0.1877, 24.4512, 0.4683, and 2.2016, respectively. The squares of correlation coefficients (R^2) to fit eqs 3 and 4 are 1.0000 and 0.9816, respectively, indicating that the tie-line data are consistently good.

Not only must the buffer species be appreciable soluble in water, but it is also important that they do not react with ions or

Table 5. Values of Parameters of Equation 1 for the 1,4-Dioxane (1) + MOBS (2) + Water (3) System at 298.15 K

a	b	c	d	10^2 SD[a]
Two Liquid Phases				
0.9472	−1.4250	0.4311	0.5094	0.78
One Liquid Phase + One Solid Phase				
0.7807	0	−1.3617	0	0.51
Two Liquid Phases + One Solid Phase				
0.8564	0	−1.5297	0	0.40

[a] SD = $(\sum_{i=1}^{N}(w_1^{cal} - w_1^{exp})^2/N)^{0.5}$, where N is the number of data points. w_1^{exp} is the experimental mass fraction of 1,4-dioxane, and w_1^{cal} is corresponding data calculated using eq 1.

Table 6. Tie-Lines Obtained (w_i, Mass Fraction) in the Two-Liquid Region for the Ternary System of 1,4-Dioxane (1) + MOBS (2) + Water (3) at 298.15 K under Atmospheric Pressure

organic phase			aqueous phase		
w_1^{II}	w_2^{II}	w_3^{II}	w_1^{I}	w_2^{I}	w_3^{I}
0.7702	0.0105	0.2193	0.3218	0.2707	0.4075
0.7753	0.0138	0.2108	0.3169	0.2835	0.3996
0.7468	0.0229	0.2303	0.3718	0.2205	0.4077

molecules present in the solution.[29] The apparent transfer energy of a buffer from water (w) to an aqueous 1,4-dioxane or ethanol solutions ($\Delta G'_{tr}$) is given by[13,30] eq 5, where $S_{B,w}$ and $S_{B,ws}$ are the solubility of buffer in water and in aqueous solution of the organic solvent on the molarity scale, respectively.

$$\Delta G'_{tr} = RT \ln\left(\frac{S_{B,w}}{S_{B,ws}}\right) \quad (5)$$

Since $\Delta G'_{tr}$ is, by definition, free of solute−solute interactions, it provides information regarding solute−solvent interactions. In Table 7, the $\Delta G'_{tr}$ values are positive (unfavorable interaction) and increase with increasing the organic solvent content of the solvent mixtures. Moreover, the $\Delta G'_{tr}$ values (unfavorable interactions) of MES with ethanol are greater than those of 1,4-dioxane except at 0.7 and 0.8 mass fractions. In contrast, the values of MOBS with ethanol are lower than those of MOBS with

dx.doi.org/10.1021/je200244p |J. Chem. Eng. Data 2011, 56, 4436–4443

Table 7. Apparent Transfer Free Energies ($\Delta G'_{tr}$) and ($-CH_2-CH_2-$) Group Contribution of Apparent Transfer Free Energy ($\Delta g'_{tr}$) of MES and MOBS from Water to Aqueous 1,4-Dioxane and Ethanol Solutions at 298.15 K

	$\Delta G'_{tr}$/J·mol^{-1}				$\Delta g'_{tr}$/J·mol^{-1}	
	1,4-dioxane		ethanol		($-CH_2-CH_2-$)	
($w_{org.solv}$)[a]	MES	MOBS	MES	MOBS	1,4-dioxane	ethanol
0.1	398.27	130.18	669.54	94.19	−268.09	−575.36
0.2	926.14	333.09	1533.25	283.27	−593.05	−1249.98
0.3	1801.09	757.48	2372.31	599.05	−1043.61	−1773.26
0.4	2583.80	phase separation	3537.90	950.36	phase separation	−2587.54
0.5	3927.09		4823.31	1695.33		−3127.98
0.6	5671.10		6225.01	2638.90		−3586.11
0.7	8176.49		7645.47	4843.57		−2801.90
0.8	10726.21		11064.52	8372.08		−2692.45
0.9	—		—	12886.20		—

[a] $w_{org.solv}$ = mass fraction of organic solvent.

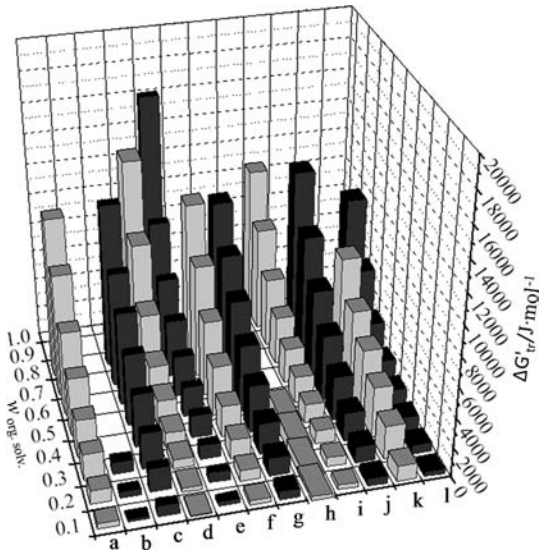

Figure 5. Apparent transfer free energy ($\Delta G'_{tr}$) of MES, MOBS, TRIS, TAPS, TAPSO, and TABS from water to aqueous 1,4-dioxane and ethanol solutions at 298.15 K: $w_{org.solv}$ = mass fraction of organic solvent. The symbols (a) and (b) represent, respectively, MES and MOBS in the 1,4-dioxane + water mixture; the symbols (c) and (d) represent, respectively, MES and MOBS in ethanol + water mixture; the symbols (e), (f), (g), and (h) represent, respectively, TRIS, TAPS, TAPSO, and TABS in 1,4-dioxane + water mixture; and the symbols (i), (j), (k), and (l) represent, respectively, TRIS, TAPS, TAPSO, and TABS in ethanol + water mixture. The $\Delta G_{tr}'$ values of TRIS, TAPS, TAPSO, and TABS in aqueous solutions of 1,4-dioxane and ethanol are obtained from refs 14 and 17, respectively.

1,4-dioxane, over the concentration range of 0.1 to 0.3 in mass fraction.

Figure 5 shows the comparison of the $\Delta G'_{tr}$ values of MES and MOBS with related biological buffers: 2-amino-2-hydroxymethyl-propane-1,3-diol (TRIS), TAPS, 2-hydroxy-3-[tris(hydroxymethyl)methylamino]-1-propanesulfonic acid (TAPSO), and TABS. Among of these important biological buffers, MES, TAPS, and TAPSO have highly unfavorable interactions with 1,4-dioxane or ethanol. We also calculated ($-CH_2-CH_2-$) group contributions by the subtraction of $\Delta G'_{tr,MES}$ from $\Delta G'_{tr,MOBS}$ values, as illustrated in Scheme 1. From Table 7, the apparent transfer energies (Δg_{tr}) of ($-CH_2-CH_2-$) group are negative over the entire experimental concentration range due to the hydrophobic interaction with the organic solvents.

CONCLUSIONS

The densities of MES and MOBS in 1,4-dioxane + water and ethanol + water were measured at 298.15 K over a wide composition range. The solubilities of these buffers in the same solutions have been determined using the density measurements at 298.15 K. The solubilities of MES and MOBS decrease with an increase of 1,4-dioxane and ethanol concentrations, and the solubility of MOBS in water is greater than that of MES. It was observed that MOBS induced liquid−liquid phase splitting in 1,4-dioxane + water mixtures over the concentrations of 1,4-dioxane from 0.4 to 0.9 in mass fraction. The phase diagram and the tie-lines of the 1,4-dioxane + MOBS + water system were measured at 298.15 K. The experimental binodal data were correlated using an empirical equation and the excluded volume theory. The Othmer−Tobias equation and the Bancroft equation were used to prove the reliability of the tie-line data. The apparent free energy of transfer ($\Delta G'_{tr}$) of these buffers from water to aqueous 1,4-dioxane and ethanol solutions at 298.15 K were calculated from the solubility data. The $\Delta G'_{tr}$ values of MES and MOBS are compared to those $\Delta G'_{tr}$ values of TRIS, TAPS, TAPSO, and TABS buffers, revealing that MES, TAPS, and TAPSO have highly unfavorable interactions with 1,4-dioxane or ethanol and the ($-CH_2-CH_2-$) group contributions for the apparent transfer energies ($\Delta g'_{tr}$) are negative (favorable interaction).

AUTHOR INFORMATION

Corresponding Author

*Tel.: +886-2-2737-6626; fax: +886-2-2737-6644. E-mail address: mjlee@mail.ntust.edu.tw (M.J. Lee).

Funding Sources

The authors are grateful for financing provided by the National Science Council, Taiwan, through Grant No. NSC97-2214-E-011-049-MY3 and NSC99-2811-E-011-023.

■ ACKNOWLEDGMENT

The authors thank Dr. Ho-mu Lin for valuable discussions.

■ REFERENCES

(1) Good, N. E.; Winget, G. D.; Winter, W.; Connolly, T. N.; Izawa, S.; Singh, R. M. M. Hydrogen Ion Buffers for Biological Research. *Biochemistry* **1966**, *5*, 467–477.

(2) Ferguson, W. J.; Braunschweiger, K. I.; Braunschweiger, W. R.; Smith, J. R.; McCormick, J. J.; Wasmann, C. C.; Jarvis, N. P.; Bell, D. H.; Good, N. E. Hydrogen Ion Buffers for Biological Research. *Anal. Biochem.* **1980**, *104*, 300–310.

(3) Kaushal, V.; Barnes, L. D. Effect of Zwitterionic Buffers on Measurement of small Masses of Protein with Bicinchoninic Acid. *Anal. Biochem.* **1986**, *157*, 291–294.

(4) Thiela, T.; Liczkowskib, L.; Bissena, S. T. New Zwitterionic Butanesulfonic Acids that Extend the Alkaline Range of Four Families of Good Buffers: Evaluation for Use in Biological Systems. *J. Biochem. Biophys. Methods* **1998**, *37*, 117–129.

(5) Blatny, P.; Kvasnicka, F.; Kenndler, E. Trace Determination of Iron in Water at the μg/L level by On-Line Coupling of Capillary Isotachophoresis and Capillary Zone Electrophoresis with UV Detection of the EDTA-Fe(III) Complex. *J. Chromatogr., A* **1997**, *757*, 297–302.

(6) Nagira, K.; Hayashida, M.; Shiga, M.; Sasamoto, K.; Kina, K.; Osada, K.; Sugahara, T.; Murakami, H. Effects of Organic pH Buffers on a Cell Growth and an Antibody Production of Human-human Hybridoma HB4C5 Cells in a Serum-free Culture. *Cytotechnology* **1995**, *17*, 117–125.

(7) Vilariño, A.; Frey, B.; Shüepp, H. MES [2-(*N*-Morpholine)-Ethane Sulphonic Acid] Buffer Promotes the Growth of External Hyphae of the Arbuscular Mycorrhizal Fungus Glomus Intraradices in An Alkaline Sand. *Biol. Fertil. Soils* **1997**, *25*, 79–81.

(8) Wolf, C.; Spence, P. L.; Pirkle, W. H.; Derrico, E. M.; Cavender, D. M.; Rozing, G. P. Enantioseparations by Electrochromatography with Packed Capillaries. *J. Chromatogr., A* **1997**, *782*, 175–179.

(9) Cifuentes, A.; Rodriguez, M. A.; Garcia-Montelongo, F. J. Separation of Basic Proteins in Free Solution Capillary Electrophoresis: Effect of Additive, Temperature and Voltage. *J. Chromatogr., A* **1996**, *742*, 257–266.

(10) Chiari, M.; Dell'Orto, N.; Casella, L. Separation of Organic Acids by Capillary Zone Electrophoresis in Buffers Containing Divalent Metal Cations. *J. Chromatogr., A* **1996**, *745*, 93–101.

(11) Rieger, C. E.; Lee, J.; Turnbull, J. L. A Continuous Spectrophotometric Assay for AspartateTranscarbamylase and ATPases. *Anal. Biochem.* **1997**, *246*, 86–95.

(12) Carr, G. R. Use of Zwitterionic Hydrogen Ion Buffers in Media for Growth Tests of Glomus Caledonium Soil. *Biol. Biochem.* **1991**, *23*, 205–206.

(13) Liu, Y.; Bolen, D. W. The Peptide Backbone Plays a Dominant Role in Protein Stabilization by Naturally Occurring Osmolytes. *Biochemistry* **1995**, *34*, 12884–12891.

(14) Taha, M.; Lee, M. J. Buffer Interactions: Solubilities and Transfer Free Energies of TRIS, TAPS, TAPSO, and TABS from Water to Aqueous Ethanol Solutions. *Fluid Phase Equilib.* **2010**, *289*, 122–128.

(15) González-Tello, P.; Camacho, F.; Blázquez, G.; Alarcòn, F. G. Liquid-Liquid Equilibrium in the System Poly(ethylene glycol) + $MgSO_4$ + H_2O at 298 K. *J. Chem. Eng. Data* **1996**, *41*, 1333–1336.

(16) Hong, G. B.; Lee, M. J.; Lin, H. M. Liquid−Liquid Equilibria of Ternary Mixtures of Water + 2-Propanol with Ethyl Acetate, Isopropyl Acetate, or Ethyl Caproate. *Fluid Phase Equilib.* **2002**, *202*, 239–252.

(17) Taha, M.; Lee, M. J. Buffer Interactions: Densities and Solubilities of Some Selected Biological Buffers in Water and in Aqueous 1,4-Dioxane Solutions. *Biochem. Eng. J.* **2009**, *46*, 334–344.

(18) Wouters, J.; Stalke, D. TAPSO at Low Temperature. *Acta Crystallogr., Sect. C* **1996**, *52*, 1684–1686.

(19) Wouters, J.; Häming, L.; Sheldrick, G. HEPES. *Acta Crystallogr., Sect. C* **1996**, *52*, 1687–1688.

(20) Cohn, E. J. Influence of the Dielectric Constant in Biochemical Systems. *Chem. Rev.* **1936**, *19*, 241–273.

(21) Takamuku, T.; Yamaguchi, A.; Matsuo, D.; Tabata, M.; Yamaguchi, T.; Otomo, T.; Adachi, T. NaCl-Induced Phase Separation of 1,4-Dioxane−Water Mixtures Studied by Large-Angle X-Ray Scattering and Small-Angle Neutron Scattering Techniques. *J. Phys. Chem. B* **2001**, *105*, 10101–10110.

(22) Guan, Y.; Lilleyand, T. H.; Treffry, T. E. A New Excluded Volume Theory and Its Application to the Coexistence Curves of Aqueous Polymer Two-Phase Systems. *Macromolecules* **1993**, *26*, 3971–3979.

(23) Wang, Y.; Mao, Y.; Han, J.; Liu, Y.; Yan, Y. Liquid Liquid Equilibrium of Potassium Phosphate/Potassium Citrate/Sodium Citrate Ethanol Aqueous Two-Phase Systems at (298.15 and 313.15) K and Correlation. *J. Chem. Eng. Data* **2010**, *55*, 5621–5626.

(24) Wang, Y.; Yan, Y.; Hu, S.; Han, J.; Xu, X. Phase Diagrams of Ammonium Sulfate Ethanol/1-Propanol/2-Propanol Water Aqueous Two-Phase Systems at 298.15 K and Correlation. *J. Chem. Eng. Data* **2010**, *55*, 876–881.

(25) Wang, Y.; Hu, S.; Han, J.; Yan, Y. Measurement and Correlation of Phase Diagram Data for Several Hydrophilic Alcohol Citrate Aqueous Two-Phase Systems at 298.15 K. *J. Chem. Eng. Data* **2010**, *55*, 4574–4579.

(26) Han, J.; Pan, R.; Xie, X.; Wang, Y.; Yan, Y.; Yin, G.; Guan, W. Liquid Liquid Equilibria of Ionic Liquid 1-Butyl-3-Methylimidazolium Tetrafluoroborate Sodium and Ammonium Citrate Aqueous Two-Phase Systems at (298.15, 308.15, and 323.15) K. *J. Chem. Eng. Data* **2010**, *55*, 3749–3754.

(27) Zafarani-Moattar, M. T.; Hamzehzadeh, S. Liquid Liquid Equilibria of Aqueous Two-Phase Systems Containing 1-Butyl-3-methylimidazolium Bromide and Potassium Phosphate or Dipotassium Hydrogen Phosphate at 298.15 K. *J. Chem. Eng. Data* **2007**, *52*, 1686–1692.

(28) Othmer, D. F.; Tobias, P. E. Liquid-liquid extraction Data-Toluene and Acetaldehyde Systems. *Ind. Eng. Chem.* **1942**, *34*, 690–692.

(29) Perrin, D. D.; Dempsey, B. *Buffers for pH and Metal Ion Control*; John Wiley & Sons, Inc.: New York, 1974.

(30) Taha, M.; Lee, M. J. Interactions of TRIS [tris(Hydroxymethyl)-aminomethane] and Related Buffers with Peptide Backbone: Thermodynamic Characterization. *Phys. Chem. Chem. Phys.* **2010**, *12*, 12840–12850.

■ NOTE ADDED AT ASAP PUBLICATION

There was an error in equation 2 in the version published on 5/16/2011. This was fixed in the version published on 6/23/2011.